

⁷⁵As NMR-NQR study in superconducting LiFeAs

Seung-Ho Baek^{1,a}, Hans-Joachim Grafe¹, Franziska Hammerath¹, Madeleine Fuchs¹, Christian Rudisch¹, Luminita Harnagea¹, Saicharan Aswartham¹, Sabine Wurmehl¹, Jeroen van den Brink¹, and Bernd Büchner¹

Leibniz Institute for Solid State and Materials Research IFW-Dresden, PF 270116, 01171 Dresden, Germany

Received: date / Revised version: date

Abstract. We report results of ⁷⁵As nuclear magnetic resonance (NMR) and nuclear quadrupole resonance (NQR) experiments as well as ⁷Li NMR on different samples of self flux grown LiFeAs and 5% Co doped LiFeAs single crystals, and a polycrystalline LiFeAs sample. We were able to distinguish the samples by their slightly different quadrupole frequencies, ν_Q , which is a direct measure of the electric field gradient (EFG) at the As site. Interestingly, samples with a large quadrupole frequency appear to show a different Knight shift and spin lattice relaxation in the superconducting state from those with a lower ν_Q , yet all the samples are clearly superconducting. For sample S1 which has the largest ν_Q , we find constant Knight shift \mathcal{K} across T_c for a certain direction of the magnetic field and a peculiar upturn of the NQR spin lattice relaxation rate $(T_1T)^{-1}$ below T_c . In contrast, samples with a lower ν_Q exhibit the expected behavior for a singlet superconductor: a drop of \mathcal{K} and $(T_1T)^{-1}$ for both NMR and NQR below T_c . Our results show that already tiny changes in stoichiometry uncovered by slightly different NQR frequencies lead to very different behavior of the NMR parameters in the superconducting state of LiFeAs. Different possibilities will be discussed which may explain the contrasting behavior.

PACS. XX.XX.XX No PACS code given

1 Introduction

Among the recently discovered superconducting iron pnictides [1,2], LiFeAs is a rare member exhibiting superconductivity with $T_c \sim 18$ K in a stoichiometric form without dopants or pressure. Yet, the Li content in this compound is difficult to control and seems to have a large influence on the physical properties. For example, Li deficiencies of only $\sim 1\%$ greatly suppress superconductivity [3]. Probably related to the sensitivity of the Li concentration, the superconducting ground state of LiFeAs and the pairing mechanism are still under debate.

Small angle neutron scattering (SANS) and angle resolved photoemission spectroscopy (ARPES) [4,5,6] suggest that LiFeAs could be a weakly electron-phonon coupled conventional-type superconductor. However, a recent Raman scattering study did not find evidence for substantial electron-phonon-coupling and no superconductivity-induced phonon anomalies [7]. Furthermore, while the spin density wave (SDW) state is absent in LiFeAs, there is evidence that weak local moments [8] and magnetic fluctuations are still present in the normal state, putting LiFeAs close to a magnetic instability [9,10]. Theoretical analyses of the electronic band-structure find a superconducting order parameter of s_{\pm} type driven by collinear antiferromagnetic fluctuations [11]. The fully gapped s_{\pm} supercon-

ductivity is also suggested by heat transport [12], magnetic penetration depth measurements [13], and inelastic neutron scattering (INS) study [14]. On the other hand, Brydon et al. [15] proposed spin-triplet p -wave pairing in this system. Being in agreement with the theoretical argument, vortex properties [16] and H_{c2} measurements [17] for $H \parallel ab$ show a very similar behavior as in the supposedly triplet superconductor Sr_2RuO_4 , and quasi particle interference (QPI) patterns measured by scanning tunneling microscopy (STM) [18] supports an elementary p -wave symmetry, rather than singlet pairing symmetries (s^{\pm} - or d -wave).

The so far reported NMR measurements of LiFeAs powder samples indicate the existence of magnetic correlations from the analysis of the Korringa relation [19,20]. In the superconducting state, the Knight shift shows a sharp drop at T_c which is suggestive of spin-singlet superconductivity. In the only NMR study on single crystals Ma *et al.* argue that the absence of the spin density wave ordering in LiFeAs is due to off-stoichiometry and/or lattice defects, and find two different Li sites in their superconducting samples [21].

Here, we report detailed NMR and NQR results on three single crystal LiFeAs samples, as well as on a 5% Co doped single crystal, and a polycrystalline LiFeAs sample. We show that the NQR frequency is highly sensitive to the Li content, and that samples with tiny differences in stoichiometry can be distinguished by their differ-

^a e-mail: sbaek.fu@gmail.com

ent quadrupole frequencies. A doping dependence of the quadrupole frequency has already been found in other iron pnictides [22], and similar changes of ν_Q with Co doping in LiFeAs indicate that also Li deficiencies change the doping level of the samples. Interestingly, samples with a large quadrupole frequency appear to show a different Knight shift and spin lattice relaxation in the superconducting state from those with a lower ν_Q . Sample S1 which has the largest ν_Q , exhibits a constant Knight shift \mathcal{K} across T_c for a certain direction of the magnetic field and a peculiar upturn of the spin lattice relaxation rate $(T_1T)^{-1}$ below T_c . In contrast, samples with a lower ν_Q exhibit a drop of \mathcal{K} and $(T_1T)^{-1}$ below T_c . Our results show that already tiny changes in stoichiometry uncovered by slightly different NQR frequencies lead to very different behavior of the NMR parameters in the superconducting state of LiFeAs. The tiny differences in stoichiometry and their large impact on the superconducting properties may also account for the contradicting results reported so far.

2 Sample preparation and Experimental details

The LiFeAs single crystals were grown by a self-flux method using a molar ratio of Li:Fe:As = 3:2:3 similar to ref. [23]. The stoichiometry of the samples has been checked by inductively coupled plasma mass spectroscopy (ICPMS). 20 mg of the LiFeAs single crystal were dissolved in a leak free glass ampoule in nitric acid. The molar ratio Li:Fe:As is found to be 0.99:1.00:1.00, consistent with a stoichiometric LiFeAs composition [23]. ARPES measurements performed on a LiFeAs single crystal from the same batch were found to be in agreement with an exact stoichiometry [5].

The susceptibility of our samples exhibits a sharp superconducting transition at $T_c \sim 18$ K [23,4]. A clear anomaly at T_c in the specific heat measurement [24], and the large residual resistance ratio (RRR) [23,25], with the lowest residual resistivity observed so far in iron pnictides [26,27,28] indicate that the samples are clean superconductors. Furthermore, STM measurements yield a defect concentration $< 1\%$ [18]. Another method to check the sample quality is the measure of the linewidth of a NQR spectrum or, equivalently, of the satellite transitions ($I_z = -3/2 \leftrightarrow -1/2$ and $I_z = +1/2 \leftrightarrow +3/2$) of a NMR spectrum, because those measure directly the distribution of the electric field gradient (EFG) which is caused by disorder or defects in the sample, while the broadening of the central transition ($I_z = -1/2 \leftrightarrow +1/2$) is dominantly magnetic in origin. As we will show below, all samples exhibit very narrow linewidth of both ^{75}As NQR lines and ^7Li NMR satellites which prove the absence of large amounts of defects in our samples and a stoichiometry of close to 1:1:1.

^{75}As (nuclear spin $I = 3/2$) NMR/NQR, and ^7Li ($I = 3/2$) NMR measurements were carried out in five different LiFeAs samples: four single crystalline samples: S1, S2, S3, and Co 5%-doped LiFeAs, and a polycrystalline sample, where the single crystals S1, S2, and S3 are from the

same batch. Due to the extreme sensitivity of the samples to air and moisture, all the samples were carefully sealed into quartz tubes filled with Ar gas. It could happen that thermal cycling damages the sealing of the quartz tubes that contain the sample, so that, if the sample probe has to be taken out of the cryostat, the sample is easily degraded by contact with air. For this reason we could not obtain full data sets for all of the samples since the NMR and NQR signals become negligibly weak in a sample which had contact with air.

Since the local symmetry at the ^{75}As is axial (tetragonal), the nuclear quadrupole frequency ν_Q can be determined directly from the resonance frequency of the NQR spectrum for the ^{75}As and by the splitting of the satellites for the ^7Li . The Knight shift was obtained by measuring the central transition. The nuclear spin-lattice relaxation rates T_1^{-1} were measured by saturation and inversion recovery methods. For exact orientation of the crystals with respect to the static magnetic field a single axis goniometer has been used for most of the measurements.

3 Experimental Results

3.1 ^{75}As NQR

For the ^{75}As in a non-cubic environment, the four-fold degeneracy of the nuclear spin of $I = 3/2$ is partially lifted by the interaction between the nuclear quadrupole moment Q and the surrounding EFG, eq , which allows a NQR resonance at a frequency given by $\nu_Q \equiv e^2qQ/h$ where h is Planck's constant and e the electron charge. We find a very narrow NQR line near 21.5 MHz at room temperature, as shown in the inset of Fig. 1. The ^{75}As NQR spectra have a width ranging from 60 kHz (S2) to 80 kHz (S1) at room temperature, which is a factor of 2-3 narrower than 170 kHz reported earlier in powder samples of LiFeAs [20], and even significantly smaller than the values reported for other undoped (non-superconducting) iron pnictides: 100 kHz from NMR satellites in BaFe_2As_2 [29], 308 kHz and 385 kHz in La- and SmOFeAs, respectively [22], and 480 kHz in CaFe_2As_2 [30]. This is even more surprising regarding the high quadrupole frequency of LiFeAs with respect to the other iron pnictides, and indicates the high homogeneity of all of our single crystals.

The temperature dependences of the nuclear quadrupole frequency ν_Q of the ^{75}As are shown in Fig. 1. The results obtained in the polycrystalline sample and the 5% Co doped single crystal sample are also compared. We find that ν_Q , or the EFG eq , varies with the samples investigated. Despite the different ν_Q at a given temperature, the temperature dependences of ν_Q of all the samples are very similar among one another, i.e., ν_Q decreases with decreasing T , being saturated at low temperatures. Such a strong temperature dependence of ν_Q is commonly observed in iron pnictides [29,31], and is attributed to mostly electronic effects due to complicated multi-orbitals of the iron ion ($3d^6$), since the lattice (thermal vibration) contribution, usually, leads to an opposite (and very weak) temperature dependence. However, we can distinguish the

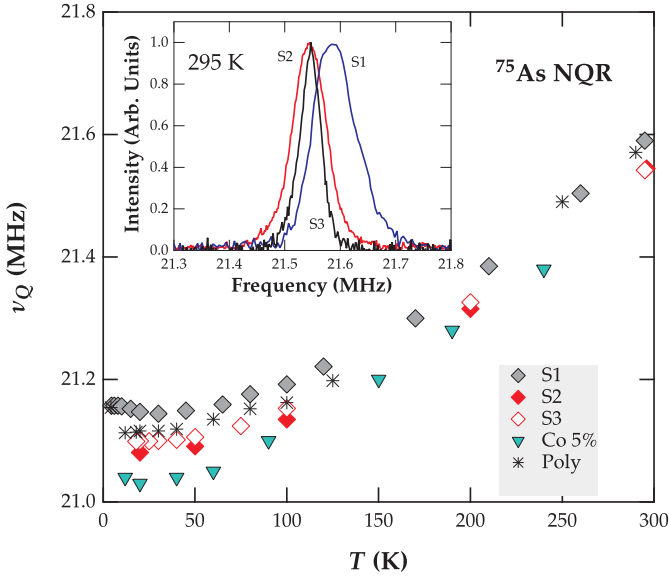


Fig. 1. The quadrupole frequency, ν_Q , decreases with decreasing temperature and almost saturates at low temperatures. While the temperature dependences of ν_Q of all the samples are similar, the values of the sample S1 are noticeably larger than those of the samples S2 and S3, as clearly shown in the inset. For comparison, $\nu_Q(T)$ for polycrystalline and Co-doped samples are shown, too. Note that the linewidth is also strongly sample-dependent, yielding 80, 60, and 40 kHz for S1, S2, and S3, respectively at room temperature.

samples clearly by their different values at a given temperature, which resembles a doping dependence similar to other pnictides [22,32] even though samples S1-S3 are from the same batch, and should have the same composition according to ICPMP and ARPES [23,5]. Interestingly, we observe that $\nu_Q(T)$ of the polycrystalline sample is very similar to that of S1, while $\nu_Q(T)$ of the Co-doped sample is even below those of S2 and S3. It appears that samples with a larger ν_Q reveal a peculiar temperature dependence of the relaxation rates and/or the Knight shift in the superconducting state, as shown below, whereas samples with a lower ν_Q show more normal behaviors, as expected in typical spin-singlet superconductors. We note that $\nu_Q(T)$ of the powder samples obtained by Li et al. [20] appears to be close to our Co-5% doped single crystal.

Fig. 2 shows the ^{75}As NQR measurement of the spin lattice relaxation rate divided by temperature, $(T_1T)^{-1}$. For all samples, $(T_1T)^{-1}$ slightly decreases with decreasing T and approaches a constant value below ~ 150 K down to T_c . Below T_c , however, the temperature dependence of $(T_1T)^{-1}$ varies among the samples. Due to the opening of the superconducting gap, the electron density of states at the Fermi level to which $(T_1T)^{-1}$ is proportional, is reduced rapidly, and thus $(T_1T)^{-1}$ is expected to decrease accordingly. While S3 exhibits such a rapid drop at T_c , S1 does not. Nevertheless, the fact that the upturn occurs at T_c suggests that the unusual behavior is associated with superconductivity, as will be discussed below in comparison to the NMR $(T_1T)^{-1}$. For the Co-

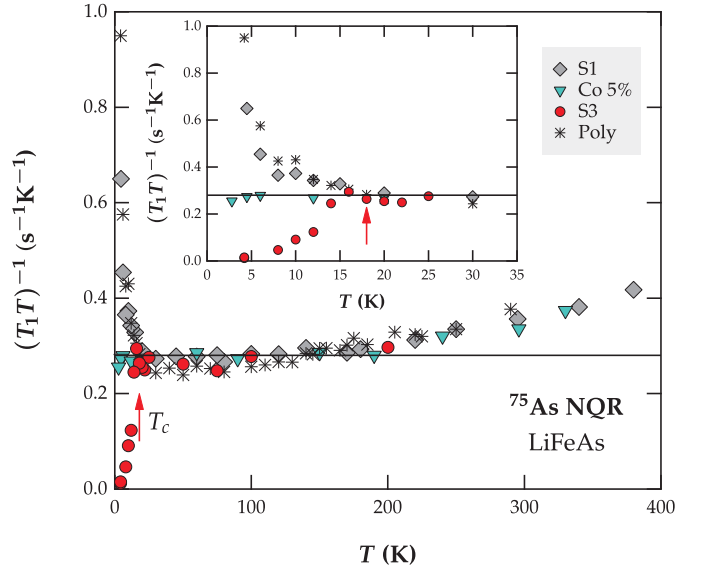


Fig. 2. ^{75}As NQR spin-lattice relaxation rates divided by T , $(T_1T)^{-1}$, as a function of T in zero field. While $(T_1T)^{-1}$ of all four samples are essentially the same above T_c , those change drastically below T_c . For both the single crystal S1 and the polycrystalline sample, $(T_1T)^{-1}$ rises below T_c . 5% Co-doping suppresses the enhancement below T_c , but still without a decrease. On the contrary, data from another single crystal S3 reveals a rapid drop, as expected in the superconducting state.

doped sample, the enhancement of $(T_1T)^{-1}$ is suppressed, while maintaining the constant value from above T_c . The polycrystalline sample also shows a strong enhancement of $(T_1T)^{-1}$ below T_c , similar to that of S1. In all cases, superconductivity has been confirmed at the same time by a strong change in the resonance frequency of the NMR circuit, which is proportional to the ac susceptibility of the sample. We note that both S1 and the polycrystalline sample which reveal a similar behavior of $(T_1T)^{-1}$ possess larger ν_Q values than the other samples, as shown in Fig. 1. Tentatively, this trend may suggest that the strength of the EFG has a relationship with the underlying physics which may cause the different behaviors of $(T_1T)^{-1}$ in the superconducting state.

3.2 ^7Li NMR spectra

Fig. 3 shows ^7Li NMR spectra including the two satellites obtained for the crystal S3. At 200 K, the spectra for both directions along c and ab reveal very sharp lines which allow us to determine $\nu_Q = 33$ kHz accurately. This value is also consistent with the value of $\nu_Q = 34$ kHz estimated by Jeglič et al. [19] by an echo decay measurement. The almost identical linewidth of central and satellite lines indicates that the broadening mechanism is mainly magnetic, and the distribution of the EFG is negligibly small. At low temperatures, the ^7Li spectra broaden significantly, unlike the ^{75}As NMR-NQR spectrum whose linewidth increases only for S1 at low temperatures. This indicates that the

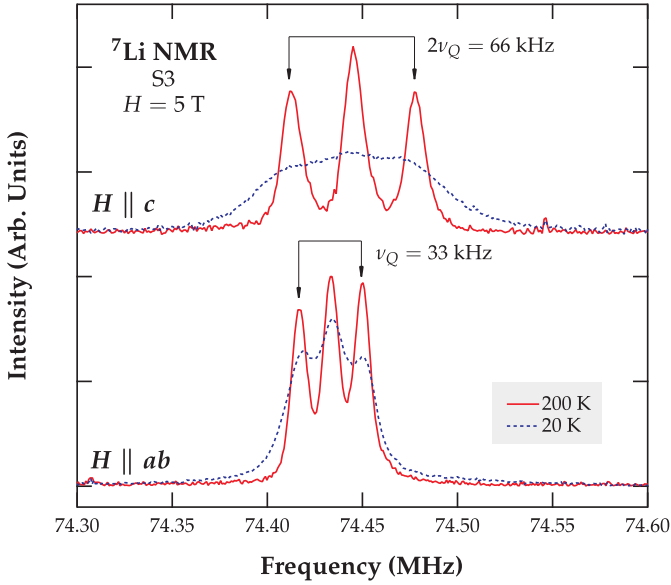


Fig. 3. ^{7}Li NMR spectra at 200 K and 20 K at $H = 4.9994$ T, with the ^{7}Li quadrupole frequency, $\nu_Q = 33$ kHz. The separation between the satellite lines for $H \parallel c$ corresponds to $2\nu_Q$, as expected in the tetragonal symmetry (the asymmetry parameter $\eta = 0$). The linewidth, which is the same for central and satellite lines, for $H \parallel ab$ ($H \parallel c$) increases from 9 kHz (11 kHz) at 200 K to 20 kHz (40 kHz) at 20 K.

^{7}Li nuclei experience quasi-static spin fluctuations at low temperatures, particularly for H along the c axis.

We emphasize that our ^{7}Li NMR spectra assure that there is only one single Li site in our crystals. This is in stark contrast with the crystals used by Ma *et al.* [21] where two ^{7}Li resonances are observed, indicating the presence of inequivalent Li sites in their crystals. Therefore our results are not consistent with the claim that the absence of magnetism is due to the off-stoichiometry or defects. Rather, we argue in this paper that the stoichiometry is a critical parameter governing the nature of magnetism and superconductivity in LiFeAs.

3.3 ^{75}As NMR Knight shifts

Fig. 4 (a) shows the T -evolution of the ^{75}As NMR central line of the single-crystal S1 measured with H parallel to the ab -plane. At high temperatures, the spectrum shifts down with decreasing T , and approaches a constant frequency below ~ 50 K. Unexpectedly, we observed that the spectrum (drawn with thick lines below T_c) maintains the resonance frequency in the superconducting state down to 4.2 K. This behavior drastically changes when H is rotated out of the ab -plane by $\sim 2^\circ$ – now the ^{75}As NMR line shows visible shifts below T_c , see Fig. 4 (b). Nevertheless, this indicates that the sample is superconducting.

Due to the large NQR frequency ν_Q , there should be a substantial shift of the central transition for $H \parallel ab$ that is strongly angle dependent, due to the second order quadrupole effect. In an uniaxial symmetry, which we confirmed by ^{7}Li NMR spectra, the second order quadrupole

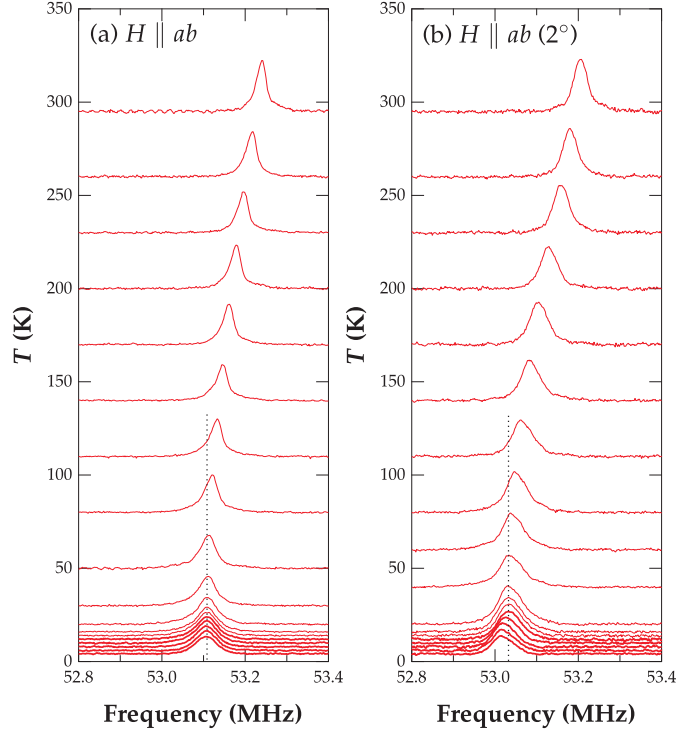


Fig. 4. ^{75}As NMR spectra of the central transition ($I_z = 1/2 \leftrightarrow -1/2$) at an external field of $H = 7.0494$ T as a function of temperature for the single crystal S1. Spectra in the superconducting state are shown as thick lines. (a) Spectra for $H \parallel ab$. Note that the resonance frequency of the spectra does not change upon going through T_c . (b) Same as in (a), but with tilting the sample by 2° . Although the temperature dependence of the shift above T_c is similar to the case of the exact alignment, the resonance frequency drops at $T_c(H) \sim 13$ K, indicating a vanishing spin susceptibility.

shift for a nucleus with spin $I = 3/2$ is given by [33]

$$\Delta\nu(\theta) = \frac{3\nu_Q^2}{16\gamma_n H} (1 - \cos^2 \theta)(1 - 9 \cos^2 \theta), \quad (1)$$

where θ is the angle between the tetragonal c axis and H .

$\Delta\nu(\theta)$ has been subtracted from the total shift of the NMR lines to extract the Knight shift shown in Fig. 5. In our case, the extreme sensitivity of $\Delta\nu$ to θ caused by the large ν_Q is indeed a benefit since one can take advantage of it in order to align the sample with great accuracy. In particular, it is very useful for $H \parallel ab$, since $\Delta\nu$ is simply the maximum when $\theta = 90^\circ$. Furthermore, we confirmed by exact diagonalization of the nuclear Hamiltonian the validity of the second order correction.

The resulting Knight shift \mathcal{K} shown in Fig. 5(a) decreases slowly upon lowering the temperature, flattening out at around 50 K, being in agreement with the results reported previously [20,19], as already reflected in the raw data (see Fig. 4). The total Knight shift \mathcal{K} consists of a spin and an orbital contribution, $\mathcal{K} = \mathcal{K}_{\text{spin}} + \mathcal{K}_{\text{orb}}$, where the latter involves the orbital motion of the conduction electrons and is usually temperature independent. Here, $\mathcal{K}_{\text{spin}}$ is directly proportional to the spin suscepti-

bility, $\mathcal{K}_{\text{spin}} = A\chi_{\text{spin}}$, where A is the hyperfine coupling strength. Therefore, \mathcal{K} should vanish at $T \ll T_c$ if the spin state of Cooper pairing is singlet. Usually, the hyperfine coupling constant is extracted from plots of \mathcal{K} versus the bulk susceptibility, χ . We extracted the hyperfine coupling constants for temperatures $T > 170$ K, because below the temperature the Knight shift does not scale with the susceptibility χ due to a magnetic impurity contribution which affects only χ . For $H \parallel ab$ we obtain $A_{ab} = 6.3 \text{ T}/\mu_B$, and for $H \parallel c$ $A_c = 0.95 \text{ T}/\mu_B$. These values appear to be strongly anisotropic, compared to other iron pnictides, e.g., $A_{ab} = 3.87 \text{ T}/\mu_B$ and $A_c = 2.61 \text{ T}/\mu_B$ for isostructural NaFeAs [34] and $A_{ab} = 2.64 \text{ T}/\mu_B$ and $A_c = 1.88 \text{ T}/\mu_B$ for BaFe₂As₂ [29].

A scaling of the Knight shifts measured for different orientations and for different nuclei would indicate that all nuclei probe the same component of the spin susceptibility. Such a behavior has been found for optimally doped LaO_{0.9}F_{0.1}FeAs [35]. Instead, we find that for ^{75}As \mathcal{K}^{ab} does not give a linear relation with \mathcal{K}^c .¹ Likewise, the Knight shift of the ^7Li nucleus does not scale with the Knight shift measured at the ^{75}As for both directions. Since there are several bands crossing the Fermi level in the iron pnictides, one can expect each band to make a different contribution to the total spin susceptibility with different hyperfine couplings to different bands. Such is the case for ^{17}O NMR in Sr₂RuO₄, where the oxygen simultaneously couples to multiple bands with different temperature-dependent susceptibilities [36]. The strong angular dependence of \mathcal{K} is also observed for the ^{17}O Knight shift in Sr₂RuO₄, whose sign changes with angle at low temperatures as in our case. While the spin susceptibility χ_{spin} is always positive, the Knight shift can be negative since $\mathcal{K}_{\text{spin}}$ can be decomposed into two components: $\mathcal{K}_{\text{spin}} = A_s\chi_s + A_{\text{cp}}\chi_{\text{non-s}}$ where A_s is the direct Fermi contact hyperfine coupling to s -electrons and A_{cp} arises from core polarization of inner s -shells due to non- s electrons (p or d) [37]. Here, A_s is always positive whereas A_{cp} is always negative. Thus, if $\chi_{\text{non-s}}$ is strongly angle and temperature dependent, \mathcal{K} will change accordingly, possibly reversing its sign. Although this may catch the essential features, the whole T - and angle-dependencies of our data obtained in LiFeAs are not correctly understood quantitatively within this simple picture. This is likely due to the multi-band structure as mentioned above. In this case, the spin susceptibility from each band may have quite different response to temperature and field direction, depending on the overlap with p -orbitals of the As ion, resulting in the observed angular and temperature dependencies of the Knight shift.

Now, we focus on the temperature dependence of \mathcal{K} at low temperatures, which is shown in Fig. 5(b). Upon

going through the superconducting T_c , the Knight shift \mathcal{K}^{ab} for the sample S1 does not show any change, which was already manifested in the raw data [Fig. 4(a)].

Furthermore, in the superconducting state the behavior of \mathcal{K} changes when the field H is tilted by just 2° out of the ab plane: there is a clear drop of \mathcal{K} at T_c and it approaches to a finite value as $T \rightarrow 0$ (see Fig. 5). For an angle of 5.6° , \mathcal{K} is small and even upturns slightly below T_c , but approaches a similar value for 2° -off case, too, as $T \rightarrow 0$. The temperature dependence of \mathcal{K} for a tilting of 2° is similar to the data measured in the polycrystalline sample [19,20], and further indicates that our crystals are superconducting. In polycrystalline samples, however, one may argue that whether \mathcal{K}^{ab} is constant for precisely in-plane field is very difficult to be confirmed due to the inevitable ambiguity in assigning the singularity for $H \parallel ab$ in a powder pattern.

However, the results measured in another single crystal S2 exhibit totally different behavior. \mathcal{K} for S2 is slightly larger than for S1 above T_c , and \mathcal{K}^{ab} shows a clear drop at T_c . With tilting the crystal by 3° , a similar behavior of \mathcal{K} was observed, unlike the strong angle dependence obtained for S1. Such a strong variation of \mathcal{K} in two samples grown in the same batch is surprising, and we interpret this as an indication that LiFeAs is located in the vicinity of an instability which may cause the extreme sensitivity of the physical properties.

3.4 ^{75}As NMR and NQR linewidth

Fig. 6 shows the temperature dependence of the full width at half maximum (FWHM) for the NMR and NQR spectra. For sample S1, FWHM increases with decreasing temperature, indicating a growing of magnetic fluctuations. In contrast, FWHM of sample S2 is nearly temperature independent. Note that for technical reasons we could obtain only limited high temperature NMR data for S2 (see also Section 2). The T independent NQR FWHM supports the fact that the NMR FWHM is also T independent, especially since its absolute value is very small even at low temperatures.

In general, the sample quality is one of the factors determining the linewidth of NMR and NQR spectra. When interpreting the linewidth one has to distinguish intrinsic effects such as broadening from local magnetic moments from the effect of impurities. This can be done by comparing the temperature dependence of the linewidth of NMR and NQR spectra where the broadening from defects (mainly quadrupole effects) and local magnetic moments (magnetic effects) appear differently. In the paramagnetic phase, the local moments are fluctuating. If the inverse correlation time, $1/\tau_c$ of the fluctuations is much higher than the NMR linewidth, each nucleus sees only the time-averaged local field and the NMR line should be narrow (motional narrowing). As the fluctuations slow down, the nuclei will start to feel a distribution of local fields which broadens the NMR/NQR lines. Note that even a tiny moment size can broaden the NMR line considerably. For example, if we assume a moment size of only

¹ We do not show \mathcal{K}^c here, because we measured our samples only with a single axis goniometer. Therefore, while one can reach a perfect alignment for $H \parallel ab$, there may be small deviations for $H \parallel c$ which lead to additional second order quadrupole correction. This affects only the absolute value of \mathcal{K}^c , but not the temperature dependence which can be compared with \mathcal{K}^{ab} .

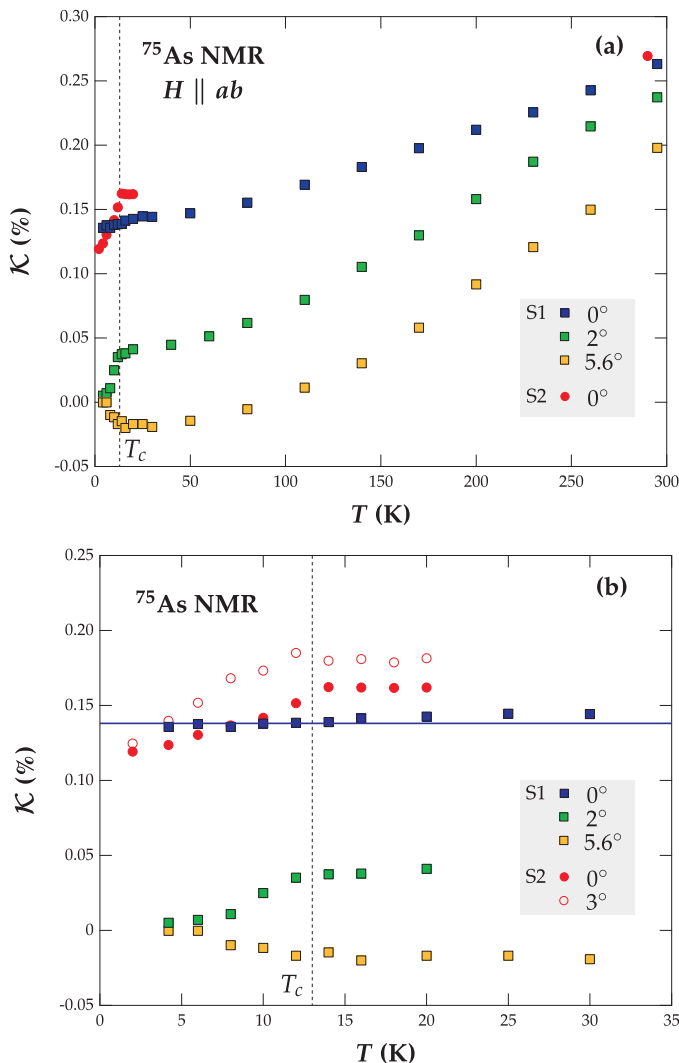


Fig. 5. (a) The Knight shift (\mathcal{K}) as a function of temperature for sample S1 for different orientations, and for S2 for $H \parallel ab$. (b) \mathcal{K} at low temperatures. For S1 and $H \parallel ab$, \mathcal{K} is constant across T_c , whereas it decreases below T_c as soon as the field is tilted out of the ab plane. In contrast, for the crystal S2, \mathcal{K} drops below T_c even for $H \parallel ab$, and the angle dependence of \mathcal{K} is not as strong as that of S1.

$10^{-4}\mu_B$, it will lead to a linewidth on the order of ~ 18 kHz, from the relation $\Delta\nu \sim H_{\text{int}} \sim A\mu$, using the hyperfine coupling $A = 6.3 \text{ T}/\mu_B$ as extracted in Section 3.3. The temperature dependence of FWHM (Fig. 6) corroborates the magnetic broadening. Disorder or defects in the sample can also lead to an enhanced magnetic broadening, but the effect of disorder is much stronger on the quadrupole broadening, and would not lead to the observed temperature dependence. However, the influence of quadrupole effects can be directly measured by NQR or by the satellite transitions ($I_z = -3/2 \leftrightarrow -1/2$ and $I_z = +1/2 \leftrightarrow +3/2$) of the NMR spectrum, whereas the central transition ($I_z = -1/2 \leftrightarrow +1/2$) is only affected by second order quadrupole effects. Any small deviations from a homogeneous charge distribution or lattice anomaly

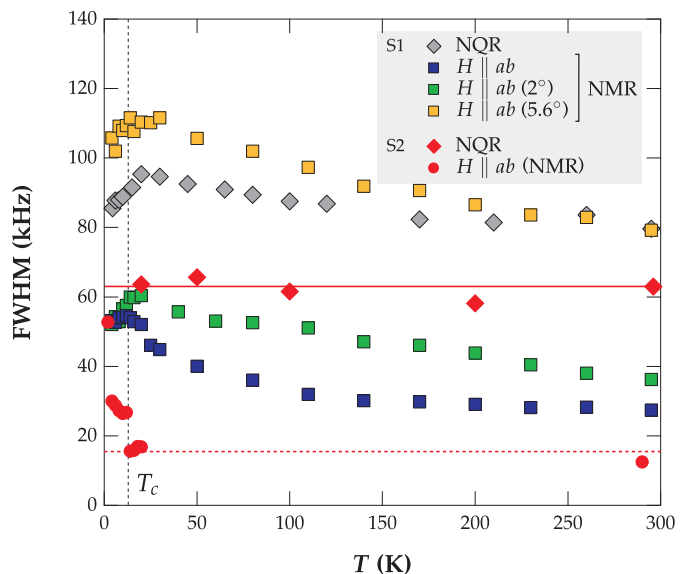


Fig. 6. FWHM as a function of temperature. For sample S1, FWHM measured by NMR and NQR increases with decreasing temperature, and shows a strong angle dependence. In contrast, for the crystal S2, FWHM is smaller than for S1 and the NQR FWHM is temperature independent. The NMR and NQR FWHM of S2 seem to be T independent as indicated by the dashed line. In the superconducting state, FWHM for S1 decreases, whereas it increases for S2.

lies such as deficiencies or defects will lead to a distribution of EFGs at the nucleus which contribute to the quadrupole linewidth. Therefore, while the narrow NQR lines of our LiFeAs single crystals is related with high homogeneity, the increase of the linewidth when approaching T_c , regardless of the rotation angle, signals that magnetic correlations progressively gain in strength upon lowering the temperature in the sample S1, whereas S2 does not show such a behavior.

We observe that the narrow line for $H \parallel ab$ rapidly broadens when H rotates out of the plane. A tilting angle of 2° already causes a noticeable broadening (Fig. 6) and for 5.6° the line broadens by a factor of three. For about 8° the width exceeds 200 kHz and \mathcal{K} is very small. Such an angle dependence could arise from a magnetic effect, where anisotropic, probably momentum-dependent, spin fluctuations are present, which are closely related to the anisotropic Knight shift \mathcal{K} . This would be in line with the presence of incommensurate, nearly ferromagnetic, spin fluctuations that emerge in microscopic calculations [15], the character of which can be strongly affected by a magnetic field. Or the angle dependence arises from a quadrupolar effect. In this case, a distribution of angles between the external magnetic field H and the direction of the principle axis of the EFG tensor V_{zz} would be needed to explain the angle dependent broadening, yet narrow NQR resonance line.

In the superconducting state, the linewidth for sample S1 unexpectedly decreases below T_c . This feature is also observed in the NQR spectra. Usually the NMR linewidth increases in the superconducting state due to vortex-related

broadening as is observed for sample S2. The origin of the decreasing linewidth just below T_c is not yet clear. Nevertheless, it indicates that the magnetic properties of the sample change at the superconducting transition temperature, namely that the spin fluctuations which lead to the broadening above T_c are strongly reduced in the superconducting state.

3.5 ^{75}As spin-lattice relaxation rates in external field

By ^{75}As NQR, we have shown that the ^{75}As $(T_1T)^{-1}$ is strongly sample dependent in the superconducting state. In order to check how an external field affects the low energy spin dynamics in the superconducting state, we measured $(T_1T)^{-1}$ by ^{75}As NMR in the two single crystals S1 and S2. As shown in Fig. 7, for the crystal S1, we observe that $(T_1T)^{-1}$ even in the normal state is enhanced compared to the NQR results (solid horizontal line). Since it is expected that the NMR results for $H \parallel c$ are equivalent to NQR ones for which the nuclei are also quantized along the c axis, the behavior is somewhat surprising, suggesting the presence of unusual, field dependent low energy spin dynamics in the system. For $H \parallel ab$, $(T_1T)^{-1}$ is further enhanced, as denoted by the dotted line. Regardless of the direction of H , the strong enhancement of $(T_1T)^{-1}$ below T_c observed in the NQR measurement (i.e., in zero field) is substantially suppressed in a magnetic field, although a sharp drop is still absent for sample S1. A similar behavior has been found in $\text{La}_{0.87}\text{Ca}_{0.13}\text{FePO}$ [38], where ^{31}P $(T_1T)^{-1}$ increases just below T_c in low magnetic fields, while high magnetic fields of about 6 T suppress this increase (see also the discussion in Section 4).

For the crystal S2, we observe contrasting results, as in the Knight shift (Fig. 5). In the normal state $(T_1T)^{-1}$ data for $H \parallel ab$ are considerably smaller than those of S1. Since NQR results were the same among all of the samples, this indicates that the spin dynamics even in the normal state become material-specific in field. In the superconducting state, a sharp drop at T_c is observed for S2, as in NQR case for S3.

An interesting observation is that $(T_1T)^{-1}$ of S1 reveals a weak but clearly visible maximum just above T_c for both directions of H . Together with the enhanced normal state $(T_1T)^{-1}$ in an external field, one can argue that the normal state spin dynamics are strongly influenced by an external field, signaling a nearby critical instability whose nature is unclear yet. Furthermore, the presence of the local maximum of $(T_1T)^{-1}$ just above T_c in field as well as the mysterious upturn of $(T_1T)^{-1}$ below T_c in zero field may indicate unusual superconductivity in LiFeAs.

4 Discussion

Our single crystals S1, S2, and S3 of LiFeAs which were grown in the same environment, exhibit significantly different static (ν_Q and \mathcal{K}) and dynamic [$(T_1T)^{-1}$] properties, particularly, in the superconducting state. Nevertheless, all the crystals are found to be of good quality

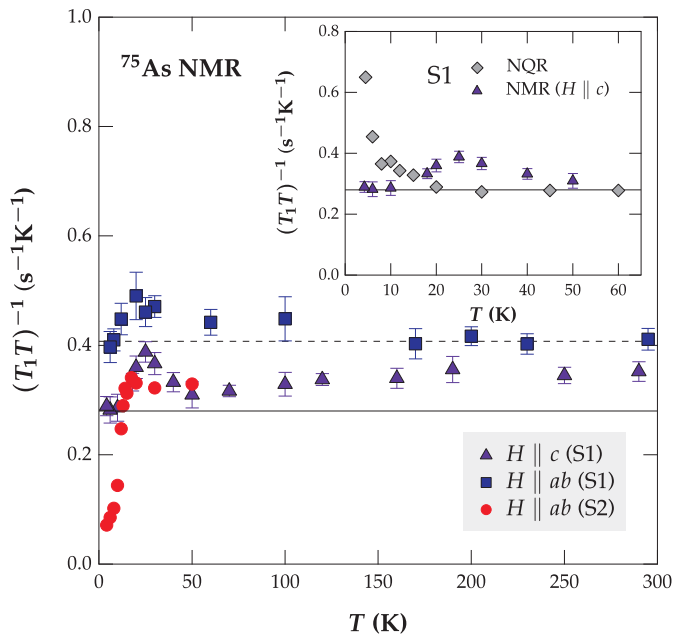


Fig. 7. ^{75}As NMR $(T_1T)^{-1}$ as a function of T measured at 7 T for the sample S1 and at 8.5 T for the sample S2. Above T_c we observe a small but visible enhancement compared to NQR results (horizontal solid line), particularly for S1. Below T_c , only the sample S2 exhibits a drop of $(T_1T)^{-1}$. Sample S3 exhibits similar temperature dependence as sample S2.

and high homogeneity as evidenced by the narrow ^{75}As NQR line and the almost equal linewidth of central and satellite ^7Li NMR lines. Although the NQR FWHM of S1 (~ 80 kHz) is much larger than that of S3 (~ 40 kHz), it is still a factor of more than 2 narrower than reported for powder LiFeAs samples [20] and significantly smaller than reported for other undoped iron pnictides (see above). Therefore, our results suggest that pure LiFeAs is located near a critical point so that its physical properties are extremely sensitive to very small perturbations such as tiny variations in stoichiometry. A similar critical doping dependence has also been reported in literature [3], where one percent of Li deficiencies largely suppress superconductivity. However, we emphasize that all of our crystals are superconducting with similar T_c . We confirmed the onset of superconductivity by a strong change in the resonance frequency of the NMR sample probe below T_c which is caused by the change of the surface resistance of the sample. Furthermore, a drop of the Knight shift for small angles off $H \parallel ab$ and the anomalous change of both the linewidth and $(T_1T)^{-1}$ below T_c indicate that sample S1 is also superconducting.

First, we discuss the different behavior of the Knight shift \mathcal{K} in the superconducting state. When a superconducting condensate consists of singlet Cooper pairs, a magnetic field cannot polarize these paired electrons unless pairs are broken up. Consequently the spin susceptibility χ_{spin} and thus \mathcal{K} vanishes [39] below T_c when $T \rightarrow 0$. This may explain the behavior that we observe in sample S2, and that is reported for powder samples of LiFeAs [19, 20]

so far. In contrast, the constant Knight shift across T_c in sample S1 for $H \parallel ab$ exhibits a behavior that would be expected for a spin-triplet superconductor where pairing does not interfere with the magnetic response of the electrons and χ_{spin} remains constant across T_c down to zero temperature. For small angles off $H \parallel ab$, however, the Knight shift decreases below T_c , suggesting that a small component of the magnetic field along the c direction leads to a transition into a state with a superconducting order parameter of different symmetry in the orbital and/or spin sector. Note that the so far reported Knight shift measurements of LiFeAs [19,20] have been performed in polycrystalline samples in which the broadening due to large second order quadrupole shift may hinder determining the intrinsic spin shift if there is a strong angle dependence of the Knight shift. Another explanation would be that the nature of superconductivity may strongly depend on the effective doping level of the samples, even though LiFeAs is considered to be a stoichiometric compound. The differences in the doping level could be visualized by the slightly different quadrupole frequencies: those samples with a high quadrupole frequency reveal the constant \mathcal{K} across T_c , whereas those samples with a lower ν_Q , including the powder sample reported in ref. [20], show a more normal behavior.

A measurement of the intrinsic spin susceptibility in the superconducting state via the Knight shift is often not straightforward and other reasons may lead to a constant \mathcal{K}^{ab} . First of all, the correction for the large second order quadrupole shift could mask a decreasing Knight shift. However, we observe that the quadrupole frequency exhibits only an insignificant temperature dependence at low T , and the constant \mathcal{K}^{ab} is already recognizable in the raw data without quadrupole correction in Fig. 4 (a). Also demagnetization effects are negligible for $H \parallel ab$ due to the plate-like shape of the crystals. Furthermore, demagnetization effects reduce the actual field in the superconductor and therefore should lead to a further decrease of the total shift \mathcal{K} below T_c . A simple heating effect of the sample by the radio frequency pulses can be excluded since we observed the decreasing Knight shift for small angles off $H \parallel ab$ and for sample S2 under similar conditions. Another reason for a constant \mathcal{K} in a singlet superconductor could be an enhanced magnetic susceptibility via strong orbital magnetism [40] or via spin-orbit scattering in the presence of disorder [41]. Such a scenario appears rather unlikely. First, the strong angular dependence of the Knight shift in the superconducting state (see Fig. 5) is incompatible with a large non-spin contribution to \mathcal{K}^{ab} , such as strong orbital magnetism. For the same reason the unchanged Knight shift through T_c cannot be explained by an impurity-based scenario. Moreover, our samples appear to be clean single crystals, even though tiny differences between the crystals have to exist.

In LiFeAs the (π,π) -nesting and static antiferromagnetism are absent [5]. Investigating theoretically the magnetic and pairing instabilities in an electronic model that incorporates the poor nesting properties and unusually shallow hole pockets of LiFeAs, Brydon and coworkers

[15] find ferromagnetic fluctuations to drive an instability toward spin-triplet p -wave superconductivity. These magnetic fluctuations are related to LiFeAs being in the vicinity of nearly ferromagnetic, incommensurate, long-range spin ordered phases, the stability of which is governed by the detailed electronic density and interaction parameters. Such a spin-triplet scenario may be supported by the constant spin susceptibility across T_c observed for $H \parallel ab$ and the increasing linewidth with decreasing temperature in sample S1, although samples S2 and S3 clearly show a spin-singlet behavior. As we have discussed above, the experimental results in single crystals S1–S3 should result from intrinsic properties rather than extrinsic ones. This suggests that different phases are competing in LiFeAs where relatively small changes due to external fields, structure or stoichiometry can cause transitions between unconventional and more conventional superconducting ground states, and may also explain other contradicting experimental results in literature (see also Section 1).

Another anomalous behavior is the strange upturn of $(T_1T)^{-1}$ in sample S1 and in the polycrystalline sample. Nakai et al. [38] suggest four different possibilities for a similar upturn in $\text{La}_{0.87}\text{Ca}_{0.13}\text{FePO}$: (i) impurity contributions which can be excluded for both compounds, as argued above. Furthermore, the relaxation curves are single exponential in LiFeAs, too, whereas impurities would lead to a multiexponential behavior of the relaxation curves. (ii) Vortex contributions to $(T_1T)^{-1}$ which can be excluded for LiFeAs since the upturn occurs in zero magnetic field (NQR). (iii) Slowing of magnetic fluctuations due to the opening of the superconducting gap. In this case, scattering of local magnetic moments with conduction electrons in the normal state enhances the energy scale of the fluctuations. In the superconducting state the scattering is suppressed due to the formation of Cooper pairs, and the local magnetic moments may slow down. As argued by Nakai et al., such a behavior has not been reported yet. (iv) Collective modes of the spin-triplet pairs could give rise to novel spin dynamics in the SC state [38, 42]. In particular, we note that the possibility (iv) may explain the observed constant Knight shift in the very same sample S1.

In order to reconcile the two different results even in the single crystals grown under the same conditions, we conjecture that the nature of spin fluctuations, which is generally thought to mediate Cooper pairs in non-BCS unconventional superconductors, could be either antiferromagnetic or ferromagnetic depending on the proximity to a ferromagnetic instability in an extremely sensitive fashion. It is also interesting to note that there is a seeming trend that the EFG and thereby the NQR frequency ν_Q are larger, when the Knight shift and $(T_1T)^{-1}$ exhibit the peculiar behaviors. This indicates a possible connection between the doping level, which could be proportional to the EFG as in other iron pnictides, and a ferromagnetic instability. Consistently, Co doping leads to a lower quadrupole frequency (EFG), and to a reduction of $(T_1T)^{-1}$ in the superconducting state, putting the Co doped sample further away from the ferromagnetic insta-

bility. This observation is also consistent with theory [11, 15], where the small hole pocket at the Γ point drives the ferromagnetic fluctuations. Regarding Co doping as electron doping, the hole pocket should shrink upon doping, thereby weakening the ferromagnetic fluctuations [43].

5 Conclusion

We have used NMR and NQR to investigate different LiFeAs samples. We find that tiny differences in the stoichiometry of the samples exist which lead to different normal state properties as well as to different superconducting properties. A possibility to distinguish the samples is the quadrupole frequency, ν_Q . Sample S1 yields a slightly higher ν_Q than sample S2, whereas ν_Q of a Co doped sample is even below that of S2. At the same time, the Knight shift of sample S1 is constant across T_c for $H \parallel ab$. Although this may suggest spin triplet superconductivity, we find that the Knight shift drops below T_c for small angles off the ab plane. On the other hand the Knight shift of sample S2 decreases in the SC state regardless of the angle which is compatible with standard singlet pairing of the Cooper pairs. The temperature dependence of the linewidth varies also with the crystals. The linewidth of sample S1 increases with decreasing temperature, indicating a growing of magnetic fluctuations, while that of sample S2 is temperature independent. Consistent with the observation of $\mathcal{K}^{ab} = \text{const.}$ across T_c could be the increasing $(T_1T)^{-1}$ in the SC state of sample S1 as well as of the polycrystalline sample which also yields a higher ν_Q . The increase of $(T_1T)^{-1}$ below T_c could originate from non-vanishing spin degree of freedom in the SC state which give rise to novel spin dynamics.

Acknowledgement

We are deeply grateful to K. Kitagawa and M. Takigawa for invaluable experimental collaboration and for sharing their data with us. The authors also thank G. Lang, C. Nacke, I. Morozov, M. Daghofer, C. Timm, and P. M. Brydon for discussion and M. Deutschmann, J. Werner, A. Voss, J. Eckert, and R. Vogel for technical support. This work has been supported by the Deutsche Forschungsgemeinschaft through FOR 538 (Grant No. BU887/4) and SPP1458 (Grant No. GR3330/2 and BE1749/13). SW acknowledges support by DFG under the Emmy-Noether program (Grant No. WU595/3-1).

References

1. Y. Kamihara, T. Watanabe, M. Hirano, and H. Hosono. *J. Am. Chem. Soc.*, 130:3296–3297, 2008.
2. M. Rotter, M. Tegel, and D. Johrendt. *Phys. Rev. Lett.*, 101:107006, 2008.
3. M. J. Pitcher, T. Lancaster, J. D. Wright, I. Franke, A. J. Steele, P. J. Baker, F. L. Pratt, W. T. Thomas, D. R. Parker, S. J. Blundell, and S. J. Clarke. *J. Am. Chem. Soc.*, 132:10467–10476, 2010.
4. D. S. Inosov, J. S. White, D. V. Evtushinsky, I. V. Morozov, A. Cameron, U. Stockert, V. B. Zabolotnyy, T. K. Kim, A. A. Kordyuk, S. V. Borisenko, E. M. Forgan, R. Klingeler, J. T. Park, S. Wurmehl, A. N. Vasiliev, G. Behr, C. D. Dewhurst, and V. Hinkov. *Phys. Rev. Lett.*, 104:187001, 2010.
5. S. V. Borisenko, V. B. Zabolotnyy, D. V. Evtushinsky, T. K. Kim, I. V. Morozov, A. N. Yaresko, A. A. Kordyuk, G. Behr, A. Vasiliev, R. Follath, and B. Büchner. *Phys. Rev. Lett.*, 105:067002, 2010.
6. A. A. Kordyuk, V. B. Zabolotnyy, D. V. Evtushinsky, T. K. Kim, I. V. Morozov, M. L. Kulić, R. Follath, G. Behr, B. Büchner, and S. V. Borisenko. *Phys. Rev. B*, 83:134513, 2011.
7. Y. J. Um, J. T. Park, B. H. Min, Y. J. Song, Y. S. Kwon, B. Keimer, and M. Le Tacon. *Phys. Rev. B*, 85:012501, 2012.
8. S. J. Zhang, X. C. Wang, R. Sammynaiken, J. S. Tse, L. X. Yang, Z. Li, Q. Q. Liu, S. Desgreniers, Y. Yao, H. Z. Liu, and C. Q. Jin. *Phys. Rev. B*, 80:014506, 2009.
9. F. L. Pratt, P. J. Baker, S. J. Blundell, T. Lancaster, H. J. Lewtas, P. Adamson, M. J. Pitcher, D. R. Parker, and S. J. Clarke. *Phys. Rev. B*, 79:052508, 2009.
10. N. Qureshi, P. Steffens, Y. Drees, A. C. Komarek, D. Lamago, Y. Sidis, L. Harnagea, H.-J. Grafe, S. Wurmehl, B. Büchner, and M. Braden. *Phys. Rev. Lett.*, 108:117001, 2012.
11. C. Platt, R. Thomale, and W. Hanke. *Phys. Rev. B*, 84:235121, 2011.
12. M. A. Tanatar, J.-Ph. Reid, S. René de Cotret, N. Doiron-Leyraud, F. Laliberté, E. Hassinger, J. Chang, H. Kim, K. Cho, Y. J. Song, Y. S. Kwon, R. Prozorov, and L. Taillefer. *Phys. Rev. B*, 84:054507, 2011.
13. K. Hashimoto, S. Kasahara, R. Katsumata, Y. Mizukami, M. Yamashita, H. Ikeda, T. Terashima, A. Carrington, Y. Matsuda, and T. Shibauchi. *Phys. Rev. Lett.*, 108:047003, 2012.
14. A. E. Taylor, M. J. Pitcher, R. A. Ewings, T. G. Per-ring, S. J. Clarke, and A. T. Boothroyd. *Phys. Rev. B*, 83:220514, 2011.
15. P. M. R. Brydon, M. Daghofer, C. Timm, and J. van den Brink. *Phys. Rev. B*, 83:060501, 2011.
16. A. K. Pramanik, L. Harnagea, C. Nacke, A. U. B. Wolter, S. Wurmehl, V. Kataev, and B. Büchner. *Phys. Rev. B*, 83:094502, 2011.
17. K. Cho, H. Kim, M. A. Tanatar, Y. J. Song, Y. S. Kwon, W. A. Coniglio, C. C. Agosta, A. Gurevich, and R. Prozorov. *Phys. Rev. B*, 83:060502, 2011.
18. T. Hänke, S. Sykora, R. Schlegel, D. Baumann, L. Harnagea, S. Wurmehl, M. Daghofer, B. Büchner, J. van den Brink, and C. Hess. *Phys. Rev. Lett.*, 108:127001, 2012.
19. P. Jeglič, A. Potočnik, M. Klanjšek, M. Bobnar, M. Jagodič, K. Koch, H. Rosner, S. Margadonna, B. Lv, A. M. Guloy, and D. Arčon. *Phys. Rev. B*, 81:140511, 2010.
20. Z. Li, Y. Ooe, X.-C. Wang, Q.-Q. Liu, C.-Q. Jin, M. Ichioka, and G.-q. Zheng. *J. Phys. Soc. Jpn.*, 79:083702, 2010.
21. L. Ma, J. Zhang, G. F. Chen, and Weiqiang Yu. *Phys. Rev. B*, 82:180501, 2010.
22. G. Lang, H.-J. Grafe, D. Paar, F. Hammerath, K. Manthey, G. Behr, J. Werner, and B. Büchner. *Phys. Rev. Lett.*, 104:097001, 2010.

23. I. Morozov, A. Boltalin, O. Volkova, A. Vasiliev, O. Kataeva, U. Stockert, M. Abdel-Hafez, D. Bombor, A. Bachmann, L. Harnagea, M. Fuchs, H.-J. Grafe, G. Behr, R. Klingeler, S. Borisenko, C. Hess, S. Wurmehl, and B. Büchner. *Cryst. Growth Des.*, 10:4428–4432, 2010.
24. U. Stockert, M. Abdel-Hafez, D. V. Evtushinsky, V. B. Zabolotnyy, A. U. B. Wolter, S. Wurmehl, I. Morozov, R. Klingeler, S. V. Borisenko, and B. Büchner. *Phys. Rev. B*, 83:224512, 2011.
25. O. Heyer, T. Lorenz, V. B. Zabolotnyy, D. V. Evtushinsky, S. V. Borisenko, I. Morozov, L. Harnagea, S. Wurmehl, C. Hess, and B. Büchner. *Phys. Rev. B*, 84:064512, 2011.
26. J. H. Tapp, Z. Tang, B. Lv, K. Sasmal, B. Lorenz, P. C. W. Chu, and A. M. Guloy. *Phys. Rev. B*, 78:060505, 2008.
27. X.C. Wang, Q.Q. Liu, Y.X. Lv, W.B. Gao, L.X. Yang, R.C. Yu, F.Y. Li, and C.Q. Jin. *Solid State Commun.*, 148:538–540, 2008.
28. Y. J. Song, J. S. Ghim, B. H. Min, Y. S. Kwon, M. H. Jung, and J.-S. Rhyee. *Appl. Phys. Lett.*, 96:212508, 2010.
29. K. Kitagawa, N. Katayama, K. Ohgushi, M. Yoshida, and M. Takigawa. *J. Phys. Soc. Jpn.*, 77:114709, 2008.
30. N J Curro, A P Dioguardi, N ApRoberts-Warren, A C Shockley, and P Klavins. *New J. Phys.*, 11:075004, 2009.
31. S.-H. Baek, N. J. Curro, T. Klimczuk, E. D. Bauer, F. Ronning, and J. D. Thompson. *Phys. Rev. B*, 79:052504, 2009.
32. S.-H. Baek, H.-J. Grafe, L. Harnagea, S. Singh, S. Wurmehl, and B. Büchner. *Phys. Rev. B*, 84:094510, 2011.
33. G. C. Carter, L. H. Bennett, and D. J. Kahan. *Metallic shift in NMR*. Pergamon, New York, 1977.
34. Kentaro Kitagawa, Yuji Mezaki, Kazuyuki Matsubayashi, Yoshiya Uwatoko, and Masashi Takigawa. *J. Phys. Soc. Jpn.*, 80:033705, 2011.
35. H-J Grafe, G Lang, F Hammerath, D Paar, K Manthey, K Koch, H Rosner, N J Curro, G Behr, J Werner, N Leps, R Klingeler, H-H Klauss, F J Litterst, and B Buchner. *New J. Phys.*, 11:035002, 2009.
36. T. Imai, A. W. Hunt, K. R. Thurber, and F. C. Chou. *Phys. Rev. Lett.*, 81:3006–3009, 1998.
37. A. Abragam. *The Principles of Nuclear Magnetism*. Oxford University Press, 1961.
38. Y. Nakai, K. Ishida, Y. Kamihara, M. Hirano, and H. Hosono. *Phys. Rev. Lett.*, 101:077006, 2008.
39. Kei Yosida. *Phys. Rev.*, 110:769–770, 1958.
40. A. M. Clogston, A. C. Gossard, V. Jaccarino, and Y. Yafet. *Rev. Mod. Phys.*, 36:170–175, 1964.
41. W. A. Hines and W. D. Knight. *Phys. Rev. B*, 4:893–903, 1971.
42. D. Vollhardt and P. Wölfe. *The Superfluid Phase of Helium 3*. Taylor and Francis, New York, 1990.
43. S. Aswartham, G. Behr, L. Harnagea, D. Bombor, A. Bachmann, I. V. Morozov, V. B. Zabolotnyy, A. A. Kordyuk, T. K. Kim, D. V. Evtushinsky, S. V. Borisenko, A. U. B. Wolter, C. Hess, S. Wurmehl, and B. Büchner. *Phys. Rev. B*, 84:054534, 2011.